Available online at www.sciencedirect.com

ScienceDirect

Physics Procedia 88 (2017) 282 – 289

Physics Procedia

8th International Topical Meeting on Neutron Radiography, Beijing, China, 4-8 September 2016

Edge enhancement investigations by means of experiments and simulations

E. Lehmann[a]*, M. Schulz[b], Y. Wang[c], A. Tartaglione[d]

[a]*Neutron Imaging & Activation Group, Paul Scherrer Institut, CH-5232 Villigen PSI*
[b]*FRM-2, TU München, D-85748 Garching*
[c]*CARR Research Reactor, China Insititute of Atomic Energy, Beijing, China*
[d]*CONICET, AR-8500 Bariloche, Argentina*

Abstract

Standard neutron imaging procedures are based on the "shadow" of the transmitted radiation, attenuated by the sample material. Under certain conditions significant deviations from pure transmission can be found in the form of enhancement or depression at the edges of the samples. These effects can limit the quantification process in the related regions. Otherwise, an enhancement and improvement of visibility can be achieved e.g. in defect analysis. In systematic studies we investigated the dependency of these effects on the specific material (mainly for common metals), such as the sample-to-detector distance, the beam collimation, the material thickness and the neutron energy. The beam lines ICON and BOA at PSI and ANTARES at TU München were used for these experiments due to their capability for neutron imaging with highest possible spatial resolution (6.5 to 13.5 micro-meter pixel size, respectively) and their cold beam spectrum. Next to the experimental data we used a McStas tool for the description of refraction and reflection features at edges for comparison. Even if minor contributions by coherent in-line propagation phase contrast are underlined, the major effect can be described by refraction of the neutrons at the sample-void interface. Ways to suppress and to magnify the edge effects can be derived from these findings.

Peer-review under responsibility of the organizing committee of ITMNR-8

Keywords: phase contrast, refractive index, edge enhancement, beam collimation, simulation, energy dependency

* Corresponding author. Tel.: +41-56-310-2963; fax: +41-56-310-3131.
E-mail address: Eberhard.lehmann@psi.ch

Peer-review under responsibility of the organizing committee of ITMNR-8
doi:10.1016/j.phpro.2017.06.039

1. Introduction: the edge features in neutron imaging

Neutron imaging data are obtained in transmission mode as “shadow” on a two-dimensional neutron sensitive detector where the local attenuation defines the contrast per pixel. In most cases, reverse calculations using the attenuation law can be done in order to derive information about composition, thickness or density of the investigated object in a quantitative way. A typical example of a flat sample is given in Fig. 1 for a dried fish, illustrating the state-of-the-art in neutron imaging with respect to contrast, spatial resolution and field of view. The high sensitivity for hydrogenous materials is the reason for this impressive contrast in the neutron data.

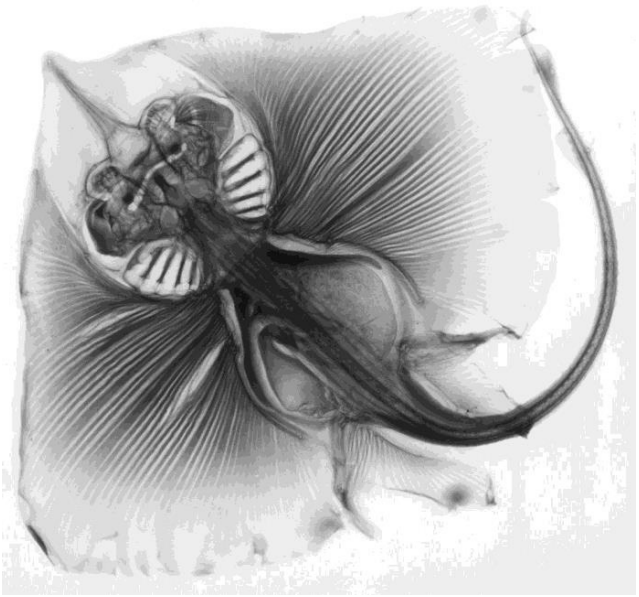

Fig. 1: Neutron transmission image of a dried fish – a ray - (sample size about 15 cm in diameter) showing many details of the organic structure, mainly caused by the attenuation in the hydrogenous material; in this setup, no phase-contrast features are induced and visible. The image was taken at the thermal beam line NEUTRA at SINQ, PSI, using a neutron sensitive imaging plate

However, under certain conditions these transmission images deviate strongly from the pure attenuation behavior. At the edges of the samples we recognize strong local contrast enhancements, as shown in Fig. 2 for the examples of metallic parts (steel, Ti).

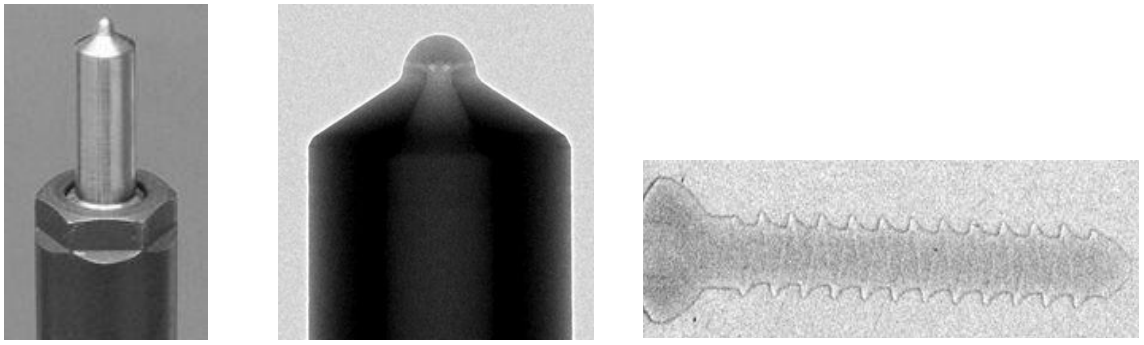

Fig. 2: Objects with edge enhancement features: left, middle: steel injection nozzle; right: Ti screw. The measurements were done at the cold neutron imaging facility ICON with a high resolution detector, sample size on the order of 20 mm, pixel size 0.0135 mm.

It has to be highlighted that edge enhancement features have become better visible in the course of increasing spatial resolution during the past years at some neutron imaging facilities.

In the case of the steel sample we have an intensity gain outside the object whereas in case of the Ti sample a decrease in intensity happens at the outer edge. These effects have relevancies in different respect: for a quantitative data interpretation the enhancement is misleading and disturbing since it does not follow the attenuation law at all; for improvement of the visualization of structures and material features (or defects) the enhancement is advantageous. The understanding of the effect is important to either suppress the enhancement for better quantification or to magnify it for best visualization.

2. Interpretational approaches

Several attempts have been done for the interpretation of edge features until now. Since they occur only under certain conditions (see below), they were not seen in the past when film methods and thermal neutrons were used and the beam collimation and spatial resolution were quite limited.

Studies at NIST were done with a highly collimated beam and the sample placed in far distance from the detector [1]. The interpretation at this time (2000) was “in-line propagation phase contrast”, similarly to the effects in X-ray studies with synchrotron sources. Since this interference approach requires a high degree of spatial coherence the beam aperture was set to 0.2 mm only. The disadvantage of this setup was the very long exposure time (on the order of hours to days).

Later, some more studies were performed [2, 3] under more relaxed beam conditions with respect to collimation and with systematics in the determination of the other setup parameters. The interpretation of the edge effects were based on the refraction approach [6] with the refraction index of neutrons as it is defined in neutron physics [4]:

$$n = 1 - \beta = 1 - \frac{\lambda^2 \cdot N \cdot b_c}{2\pi} \approx 1 - 10^{-6} \tag{1}$$

Compared to visible light, the directional changes at material interfaces are much smaller by orders of magnitudes. In this formula the deviation from 1 is described by the parameter β which depends on the wavelength λ, the material density N and the coherent scattering length b_c. These values are well known and tabulated, e.g. in [5]. Since b_c can have positive (for most materials), but also negative values (Ti, Mn, Li), the reason of the different behavior in Fig. 2 can be found easily in the refraction properties of the both materials.

However, until today it is not completely found out if the edge effects are purely given by refraction at material interfaces described by the difference in the refraction index – where a directional change of the involved neutrons takes place. On the other hand there might be diffraction contributions possible from the in-line part, based on coherent interference effects which are not easily separable from the refraction part because they end up into the same behavior and features. Therefore, we started systematic experimental studies at several neutron imaging facilities (ICON, BOA at PSI, ANTARES at TU München), accompanied by some simulations by using McStas tools [7, 8] to find out dependencies of the mentioned effects.

3. Experiments

We have investigated materials of relevance with well-known refraction properties (Al, Fe, Ni, Zr, Cu, Pb and Ti) in different configurations with respect to sample size and shape, thickness and under various beam conditions with respect to neutron energy, sample-detector distance and collimation. These experiments were performed with highest possible spatial resolution (up to 6.5 µm pixel size = 154 pixels/mm) [6] to get statistically reliable data for the comparison to simulations.

Except of Ti and Mn, most of the materials show a characteristic intensity enhancement at the outer edge, accompanied by an intensity depression towards the inside of the material, shown in Fig. 3 qualitatively. Due to the pixel size the affected region at the edge (0.3 mm) was observed in very good statistical precision. Already with a sample thickness of 0.025 mm iron the 2% intensity gain can clearly be resolved. Such kind of measurements has never been done before under the such conditions and with the precision needed.

3.1. Beam collimation

The aperture wheel at the cold imaging facility ICON provides six options for the inlet collimator close to the source: 80 mm, 40 mm, 20 mm, 10 mm, 1 mm and a Be filtered 20 mm one. In this way, the beam properties can be tuned with respect to collimation and intensity. The corresponding L/D ratio can be selected between 125 and 10,000.

We investigated an Al cuboid (thickness 10 mm) with the 4 largest collimation openings (with 1 mm no valid image was obtained in reasonable exposure time) in 100 mm distance from the detector and we obtained the results shown in Fig. 3.

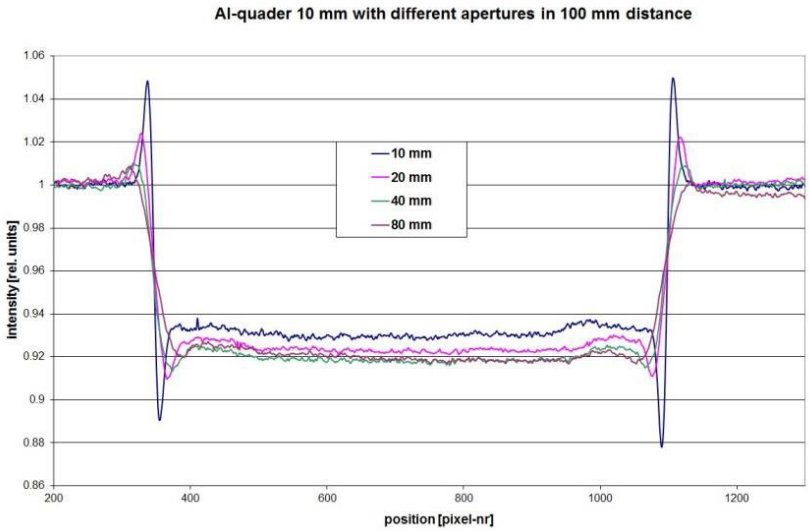

Fig. 3: Edge effects at a 10 mm Al sample placed in 100 mm distance from the detector: increasing enhancement features with higher collimation = smaller inlet apertures

The intensity of the edge effect and in particular the peak heights (see the explanations in Fig. 4) are clearly increased with smaller apertures. On the one hand, the image blurring is increased with less collimation, on the other hand some higher coherence is induced with smaller aperture.

However, with 20 mm aperture we never reach a relevant coherence condition according to (2):

$$\xi = \frac{\lambda \cdot l}{s} \tag{2}$$

With a typical wavelength λ=4 Å, a source size s (= aperture 20 mm) and a source-detector-distance l of about 10 m we obtain a coherence length ξ of 4E-7 m what is far below the resolution of the detection system. Therefore, the part of the in-line propagation phase contrast will be small under these conditions. Even with 1 mm aperture the coherence length stays on the same order of magnitude. This confirms the considerations in [6], however based on a much higher degree of precision in the experimental data.

If the coherence is not the main reason for the edge effects, refraction effects at the material borders remain as the most likely explanation. Since a higher collimation provides a part of neutron with a suitable angular distribution to fulfil the Snell's law conditions (see below). For larger apertures, the image blurring in a distance of 10 cm will dominate the refractive contribution at the edges. This will be outlined more in chapter 3.2.

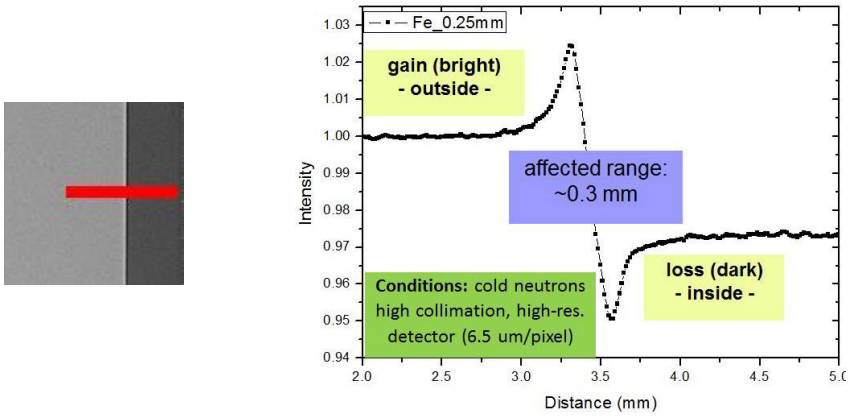

Fig. 4: Intensity distribution near the sample edge (iron of 0.25 mm thickness) investigated with highest possible spatial resolution; the profile is taken at the marked position in the left image; the terms "gain" and "loss" are explained.

3.2. Sample-detector distance

Looking to the same sample than in Fig. 3, but now varying the sample-detector distance d while the collimation conditions stay the same, we obtain the following results:

a. Visible increase of the edge effects with increasing distance to the detector as shown in Fig. 5. In close contact of the sample to the detector the edge effects are low and nearly suppressed
b. Higher (geometrical) image blurring (u_g) by the limited collimation (L/D ratio on the order of 500) of the beam according to (3); the "gain" and "loss" peaks are separating more and more

$$u_g = d/(L/D) \tag{3}$$

The sharpness reduction of the edges is increasing with the distance d while a higher L/D-ratio (length/aperture) limits the effect relatively. Following the scheme and terms in Fig. 4, the peak area in the "gain" (increase in intensity) and "loss" (decrease in intensity) region can be evaluated, as shown in Fig. 6.

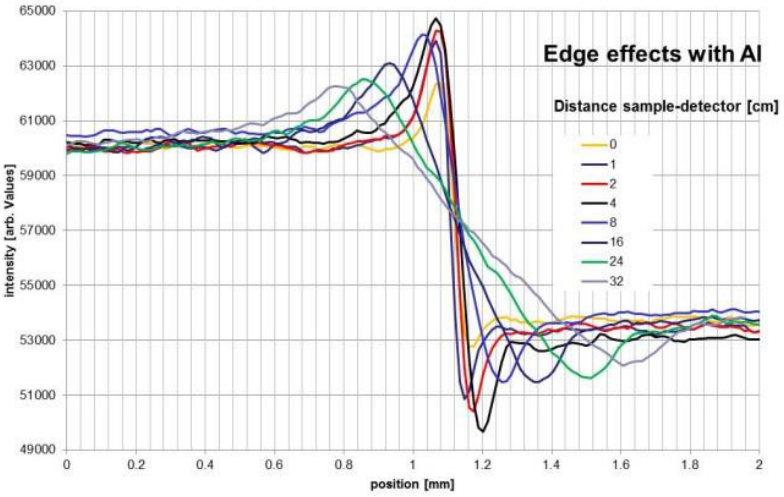

Fig. 5: Edge effects at an Al sample in dependency on the sample-detector distance under "standard conditions" with L/D=500

We evaluated the peak regions of "gain" and "loss" in more detail and derived numbers of their area. While the peak positions are spreading with the increase of the sample-detector distance (lower slope at the profile edge), the peak areas stay more or less stable for larger distances (Fig. 6). This means, the amount of involved neutrons at the edges stays about the same after a threshold is reached at about 10 mm sample-detector distance. This can be understood with considerations by Snell's law:

$$\frac{\sin\theta_1}{\sin\theta_2} = \frac{v_2}{v_1} = \frac{\lambda_1}{\lambda_2} = \frac{n_2}{n_1} \tag{4}$$

The angles θ of the incoming and outgoing beams 1 and 2 are related to the velocity v or the wavelength λ and the corresponding refractive indices. Because the refraction angle according to Snell's law (4) (n_1=1 (air); n_2=1-10^{-6} (Al)) is on the order of 0.1° only, the refracted part of the beam is not well visible in close contact with the detector due to its limited spatial resolution. In further distance, the refracted neutrons are better spread over the pixels in the detector.

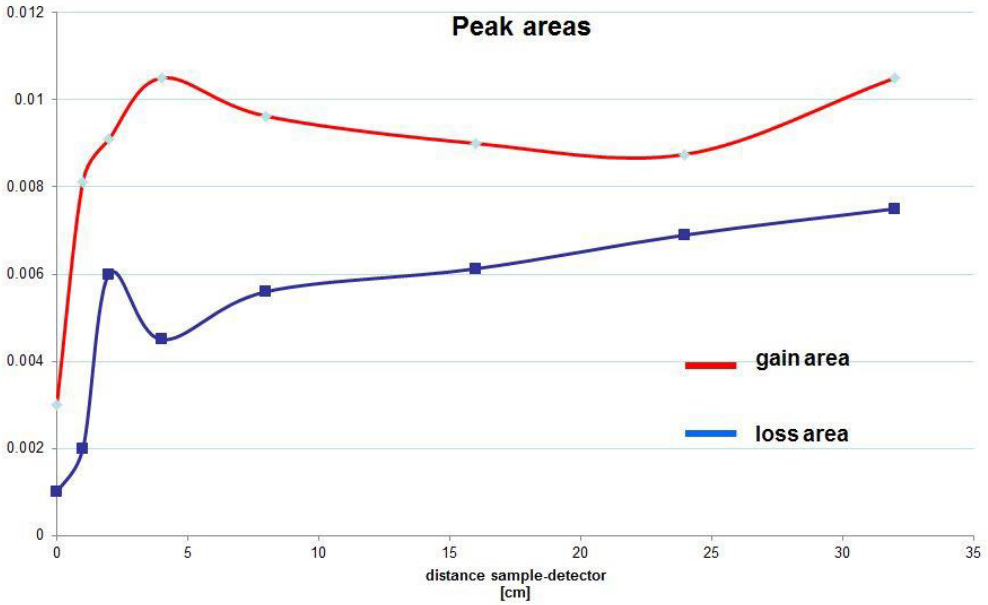

Fig. 6: Peak areas of the "gain" and "loss" regions at the edges obtained in different distances between sample and detector

3.3. Material thickness

We investigated materials with different thickness and compared the effects at the edges quantitatively by using the "peak areas" as the observable parameter. For iron, a layer of only 0.025 mm was enough to see already edge enhancement features. With increasing sample thickness, the enhancement is more and more pronounced while the attenuation in the sample becomes also higher (see the level differences in Fig. 7A left and right to the edge). There is a clear increase of the peak areas for thin layers of material, shown in the left part of this figure, underlined by the numbers for the peak areas shown in the right part. For thicker material layers, the peak areas are not further increased because the attenuation in the sample dominated the resulting signal more and more.

The futher evaluation of the gain part of the profiles near the edges of steel samples of different thickness is given in Fig. 7B, corresponding to the data in Fig. 7A. A prompt and very strong increase in the enhancement signal is visible for small thicknesses while for larger thicknesses a saturation can be found and the edge contribution stays stable.

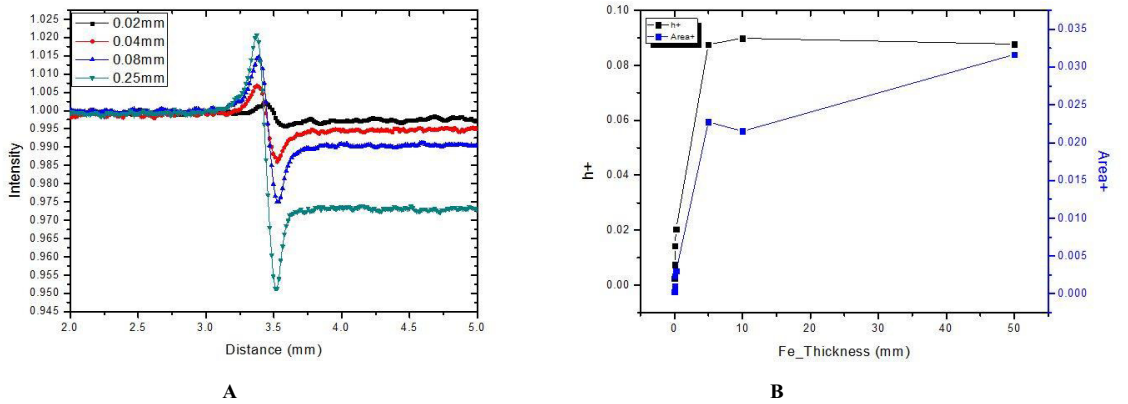

Fig. 7: Attenuation and edge enhancement study with thin iron layers where the unperturbed neutron level (open beam) outside the sample is on the left, the sample position is on the right side of the visible edge region (A); the peak height h+ and the peak area of the "gain" peaks are compared for different sample thickness (B)

3.4. Neutron energy

The investigation of the edge effects was done under variable spectral conditions at the neutron imaging beamline ANTARES, FRM-2, TU München [9]. A turbine type energy selector was used to change the mean neutron energy of the applied beam with an energy spread of 10% per wavelength from 3 to 5 Å.

We used a common iron sample of 5 mm thickness and placed it in 100 mm distance from the high resolution detector, where the enhancement and the blurring by the beam divergence are in a good ratio. The image data were evaluated at edges with broad profiles (averaging pixels for optimizing the statistics) and the "gain" and "loss" areas (see Fig. 4) were quantified. According to the experimental data shown in Fig. 8, there is the clear evidence to have increasing effects (larger areas of spread neutrons) with higher neutron wavelength.

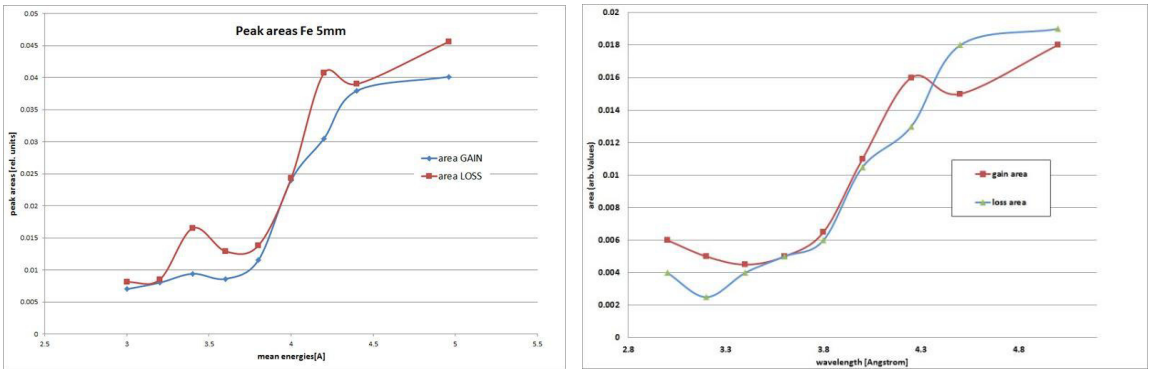

Fig. 8: Changes of the "gain" and "loss" areas (according to the scheme in Fig. 3) in dependency on the mean neutron energy: left – experimental studies for Fe (5mm) in 100 mm distance from the detector and the ANTARES beam conditions using a turbine type energy selector; right: corresponding McStas simulations

The verification of this behavior was done by means of McStas simulations, where the refraction and the reflection of neutrons is embedded by using the Snell's law conditions and the total reflection is handled correctly according to it. In this manner the conditions given by (1) are verified in a qualitative manner. More quantitative

considerations should follow with respect to the comparison to different materials where the scattering strength and the relations to b_c have to be discussed.

4. Simulations

The experimental studies were accompanied by simulations using the ray-tracing Monte Carlo code McStas [7, 8] with the implementation a specific tool for the refraction properties of the observed materials using (4), the data in (1) and the reflectivity of the materials until the limit for total reflection. Also the attenuation by absorption and scattering are handled in adequate manner. There is no tool inside McStas available until now to deal with the coherence properties of the neutrons leading to in-line phase propagation features. Therefore it is not possible to judge about such contributions from the theoretical side.

The co-authors of this report investigated several aspects of the study, in particular the energy dependency of the refraction effects, the thickness dependency and the alignment and reflectivity problems with real samples. Since the studies are not yet completed, we show in this report only some data for comparison (see above). Although most of the edge effects were verified qualitatively and explained by the simulations, the quantitative agreement is still pending. Therefore, more dedicated studies have to be performed in the next future.

5. Conclusions

Systematic studies are presented for the description and interpretation of edge effects at metallic samples of relevance by changing the conditions as collimation, sample-detector-distance, sample thickness and neutron energy using detection systems with very high spatial resolution and preferential cold neutrons where edge effects are expected to be highest.

Most of the findings can be interpreted by the refraction (and reflection) of the neutrons at the boundaries where the refraction index makes an abrupt jump (vacuum vs. material). Since the contributions by the scattering properties of the materials to the refraction index changes are very small ($1\text{-}n \sim 10^{-6}$), the features becomes best visible with the used high resolution detectors, in larger distance between sample and detector and for neutrons with longer wavelength.

The verification with a tool in McStas fits well in first order. There are some remaining differences between experiments and simulations when very thin samples are used and the collimation is extremely high. Such very “parallel conditions” does not allow any visible refraction in the model.

References

[1] B. E. Allman, P. J. McMahon, K. A. Nugent, D. Paganin, D. L. Jacobson, M. Arif & S. A. Werner, Imaging: Phase radiography with neutrons, Nature 408, 158-159 (9 November 2000) | doi:10.1038/35041626
[2] N. Kardjilov, Neutron Phase-Contrast and Polarized Neutron Tomography, Advanced Tomographic Methods in Materials Research and Engineering, p. 409-424, DOI:10.1093/acprof:oso/9780199213245.003.0014
[3] E. Lehmann, K. Lorenz, E. Streichele, P. Vontobel, Non-destructive testing with neutron phase-contrast imaging, Nuclear Instruments and Methods in Physics Research 542 (2005) 95.
[4] M. Warner and J. E. Gubernatis, Neutron refractive index: A Fermi-Huygens theory, Phys. Rev. B 32, 6347, November 1985
[5] https://www.ncnr.nist.gov/resources/n-lengths/
[6] E.H. Lehmann, G. Frei, G. Kühne, P. Boillat, The micro-setup for neutron imaging: A major step forward to improve the spatial resolution, Nuclear Instruments and Methods in Physics Research Section A: Volume 576, Issue 2, Pages 389-396
[6] M. Strobl, W. Treimer, N. Kardjilov, A. Hilger, S. Zabler, On neutron phase contrast imaging, Nuclear Instruments and Methods in Physics Research B 266 (2008) 181–186
[7] K. Lefmann and K. Nielsen, "McStas, a General Software Package for Neutron Ray-tracing Simulations", Neutron News 10, 20, (1999).
[8] https://en.wikipedia.org/wiki/McStas
[9] http://www.mlz-garching.de/antares